Title
PTEN opposes negative selection and enables oncogenic transformation of pre-B cells.

Journal
Nature medicine, 22(4)

ISSN
1078-8956

Authors
Shojaee, Seyedmehdi
Chan, Lai N
Buchner, Maike
et al.

Publication Date
2016-04-01

DOI
10.1038/nm.4062

Peer reviewed

nature medicine

PTEN opposes negative selection and enables oncogenic transformation of pre-B cells

Seyedmehdi Shojaee[1], Lai N Chan[1], Maike Buchner[1], Valeria Cazzaniga[1,2], Kadriye Nehir Cosgun[1], Huimin Geng[1], Yi Hua Qiu[3], Marcus Dühren von Minden[4], Thomas Ernst[5], Andreas Hochhaus[5], Giovanni Cazzaniga[2], Ari Melnick[6], Steven M Kornblau[3], Thomas G Graeber[7], Hong Wu[7], Hassan Jumaa[4] & Markus Müschen[1]

Phosphatase and tensin homolog (PTEN) is a negative regulator of the phosphatidylinositol 3-kinase (PI3K) and protein kinase B (AKT) signaling pathway and a potent tumor suppressor in many types of cancer. To test a tumor suppressive role for PTEN in pre-B acute lymphoblastic leukemia (ALL), we induced Cre-mediated deletion of *Pten* in mouse models of pre-B ALL. In contrast to its role as a tumor suppressor in other cancers, loss of one or both alleles of *Pten* caused rapid cell death of pre-B ALL cells and was sufficient to clear transplant recipient mice of leukemia. Small-molecule inhibition of PTEN in human pre-B ALL cells resulted in hyperactivation of AKT, activation of the p53 tumor suppressor cell cycle checkpoint and cell death. Loss of PTEN function in pre-B ALL cells was functionally equivalent to acute activation of autoreactive pre–B cell receptor signaling, which engaged a deletional checkpoint for the removal of autoreactive B cells. We propose that targeted inhibition of PTEN and hyperactivation of AKT triggers a checkpoint for the elimination of autoreactive B cells and represents a new strategy to overcome drug resistance in human ALL.

The majority of newly generated pre-B cells in the bone marrow are eliminated at the pre–B cell receptor (pre-BCR) checkpoint[1]. Critical survival and proliferation signals come from the pre-BCR; if pre-B cell clones fail to express a functional pre-BCR, then signaling output is too weak. If the pre-BCR binds to ubiquitous self-antigen (autoreactive immunoglobulin μ heavy chain; μ-HC), then pre-BCR signals are strong. Both attenuation below a minimum (such as a nonfunctional pre-BCR) and hyperactivation above a maximum (such as an autoreactive pre-BCR) threshold of signaling strength trigger negative selection and cell death. Approximately 75% of newly generated pre-B cells express an autoreactive μ-HC[2,3], highlighting the importance of stringent negative selection of autoreactive clones at the pre-BCR checkpoint. Although autoreactive pre-B cell clones are eliminated owing to the toxicity of strong pre-BCR signaling[1–3], sustained activation of PI3K-AKT signaling is sufficient to rescue B cell survival in the absence of a functional BCR[4] and is required for pre-B cell survival[5]. Likewise, germline mutations in humans that result in either loss or hyperactivation of PI3K-AKT signaling have equally deleterious effects on human early B cell development[6], suggesting that early B cells undergo selection for an intermediate level of PI3K signaling.

PTEN is a key negative regulator of the PI3K-AKT pathway and functions as a dual protein and lipid phosphatase that dephosphorylates phosphatidylinositol (3,4,5)-triphosphate (PIP_3). PTEN counteracts the activity of PI3K, which phosphorylates phosphatidylinositol (4,5)-bisphosphate (PIP_2) to generate PIP_3, the membrane anchor and ligand of AKT's pleckstrin homology (PH) domain[7]. Deletions or inactivating mutations of *PTEN* are frequently observed in all main types of human cancer (on average 8.3% among 37,898 samples studied)[8]. The common outcome of these lesions is increased membrane levels of PIP_3 and AKT hyperactivation. Genetic lesions of *PTEN* mutations also have a major role in hematopoietic malignancies. For instance, lesions in *PTEN* and in genes encoding components of the PI3K-AKT pathway are present in up to 50% of T cell lineage ALL cases[9].

RESULTS

Pten is required for initiation and maintenance of pre-B ALL *in vivo*

To study a potential role of PTEN and negative regulation of PI3K-AKT signaling, we developed *BCR-ABL1*- and $NRAS^{G12D}$-driven mouse models of pre-B ALL (**Fig. 1**). To this end, we transformed interleukin (IL)-7–dependent pre-B cells from the bone marrow of mice carrying *loxP*-flanked (floxed) *Pten* ($Pten^{fl/fl}$ and $Pten^{+/fl}$ mice)[10] with oncogenic *BCR-ABL1* or $NRAS^{G12D}$. *BCR-ABL1* represents the driver oncogene in Philadelphia chromosome–positive (Ph^+) ALL, the most common subtype of pre-B ALL in adults (~30%). RAS pathway lesions affect components encoded by *NRAS*, *KRAS*, *PTPN11* and *NF1*, and these occur in ~50% of both adult and pediatric ALL[11]. Together, *BCR-ABL1*– and $NRAS^{G12D}$-driven pre-B ALL reflect two major nonoverlapping types of human ALL (~80%). For inducible deletion of *Pten*, pre-B ALL cells were transduced with a construct expressing

[1]Department of Laboratory Medicine, University of California, San Francisco, San Francisco, California, USA. [2]Centro Ricerca Tettamanti, Clinica Pediatrica, Università di Milano-Bicocca, Monza, Italy. [3]Department of Leukemia, University of Texas M.D. Anderson Cancer Center, Houston, Texas, USA. [4]Department of Immunology, University of Ulm, Ulm, Germany. [5]Abteilung Hämatologie-Onkologie, Klinik für Innere Medizin II, Universitätsklinikum Jena, Jena, Germany. [6]Department of Pharmacology, Weill Cornell Medical College, New York, New York, USA. [7]Department of Molecular and Medical Pharmacology, University of California, Los Angeles (UCLA), Los Angeles, California, USA. Correspondence should be addressed to M.M. (markus.muschen@ucsf.edu).

Received 11 June 2015; accepted 10 February 2016; published online 14 March 2016; doi:10.1038/nm.4062

a tamoxifen (Tam)-inducible estrogen receptor empty vector control (ER^{T2}) or one expressing *Cre* (*Cre-ER*^{T2}). After selection of the transduced cells with puromycin, *Cre* was activated by Tam treatment (1 µmol/liter), which induced excision of the *loxP*-flanked *Pten* alleles and depletion of PTEN protein within 2 d (**Fig. 1a**). Notably, inducible Cre-mediated deletion of *Pten* in pre-B ALL cells resulted in the rapid cell death of leukemia cells (**Fig. 1b** and **Supplementary Fig. 1a**). To address whether loss of PTEN affected not only survival of established leukemia but also initiation of leukemia, we reversed the order and first induced deletion of *Pten* in IL7-dependent *Pten*$^{fl/fl}$ pre-B cells and subsequently induced *BCR-ABL1*–mediated transformation. Two days after induction of Cre, *Pten*$^{+/+}$ and *Pten*$^{-/-}$ pre-B cells were transduced with a construct encoding green fluorescent protein (GFP)-tagged BCR-ABL1 (*BCR-ABL1*^{GFP}). *Pten*$^{+/+}$ pre-B cells showed rapid outgrowth of *BCR-ABL1*^{GFP}-expressing clones, indicating leukemic transformation. In contrast, *Pten*$^{-/-}$ pre-B cells carrying *BCR-ABL1*^{GFP} were not susceptible to malignant transformation by *BCR-ABL1* (**Fig. 1c** and **Supplementary Fig. 1b**). These findings were recapitulated in an *in vivo* transplant setting. *BCR-ABL1*–transformed *Pten*$^{fl/fl}$ pre-B ALL cells caused a fatal leukemia in transplant-recipient mice within 18 d. Luciferase bioimaging revealed that Cre-mediated deletion of *Pten* did not interfere with engraftment of pre-B ALL cells. However, pre-B ALL cells failed to initiate fatal disease in the absence of PTEN, and the transplant recipients survived for indefinite periods of time (**Fig. 1d**). Minimal residual disease (MRD) analysis, using genomic PCR, revealed no trace of covert leukemia clones (**Supplementary Fig. 1c**).

Pten mediates feedback regulation of pre-BCR and its co-receptor CD19

To elucidate the mechanism of how the tumor suppressor PTEN, seemingly paradoxically, enables oncogenic transformation of pre-B cells, we studied gene expression changes after inducible *Pten* deletion (**Fig. 1e**). Loss of *Pten* induced expression of multiple markers of lymphocyte activation including *Cd80*, *Cd86*, *Il2ra* (also known as *Cd25*) and *Ly6a* (also known as *Sca-1*). *Pten* deletion resulted in downregulation of the IL-7 receptor (IL-7R), both at the mRNA level and in its surface expression (**Fig. 1e**,**f**). In addition, expression of genes encoding multiple components of the pre-BCR (*Ighm*, *Vpreb1* and *Syk*) and its co-receptor CD19 were all downregulated after deletion of *Pten* (**Fig. 1e**,**f**). In pre-B cells, PI3K-AKT signaling is initiated from the pre-BCR via SYK[4,5,12,13] and CD19 via recruitment of PI3K[14,15] to a YXXM motif in the cytoplasmic tail of CD19. For this reason, loss of pre-BCR and CD19 expression in response to deletion of *Pten* suggests PTEN-mediated feedback regulation of these PI3K-AKT activating receptors. Likewise, a B cell–specific deletion of *Pten* in *Cd79a*$^{tm1(cre)Reth}$;*Pten*$^{fl/fl}$ mice caused loss of CD19 expression in B lineage cells (**Fig. 1g**). Western blot analysis confirmed near-complete loss of CD19 protein expression after deletion of *Pten*, as shown by loss of both surface and intracellular expression of CD19 (**Fig. 1h**).

Deletion of Pten compromises BCR-ABL1 and NRAS-driven leukemogenesis

BCR-ABL1 and *NRAS*^{G12D}-driven ALL subtypes were dependent on PTEN function to a similar degree, as inducible, Cre-mediated deletion of *Pten* induced cell death and reduced colony-forming ability (**Fig. 2a**,**b**). Genotyping of colonies revealed that *Pten*$^{fl/fl}$ pre-B ALL clones that were able to form colonies had retained floxed *Pten* alleles despite activation of Cre. Hence, these few colonies arose from pre-B ALL clones that had evaded Cre-mediated deletion of *Pten* (**Supplementary Fig. 2**).

Pten deletion also induced G0-G1 cell cycle arrest and senescence in pre-B ALL cells (**Fig. 2c**,**d**). To assess the effect of acute ablation of *Pten* in fully established *BCR-ABL1* and *NRAS*^{G12D}-driven pre-B ALL cells *in vivo*, 100,000 *Pten*$^{fl/fl}$ pre-B ALL cells carrying tamoxifen-inducible *Cre* were injected into sublethally irradiated NOD.CB17-Prkdc^{scid}/J (NOD-SCID) recipient female mice for engraftment. Five days after transplantation of *Pten*$^{fl/fl}$ pre-B ALL cells, leukemia initiation and engraftment was confirmed by using bioluminescence imaging, and *Cre* was induced by ten consecutive daily injections of tamoxifen. Consistent with *in vitro* results, *Pten* deletion caused leukemia regression *in vivo* (**Fig. 2e**) and prolonged overall survival in the recipient mice. We conclude that *Pten* is required for both initiation and maintenance of pre-B ALL *in vivo*.

Pre-B ALL cells are exempt from genetic lesions of *PTEN*

Given the unexpected sensitivity of pre-B ALL cells to even a moderate dose reduction of *Pten*, we reassessed the concept of PTEN as a tumor suppressor in human cancer and in leukemias and lymphomas. A reanalysis of genetic lesions of *PTEN* in human cancer revealed a high frequency of mutations in solid cancer (8.3% in 37,898 samples) and hematological malignancies (8.4% in 2,548 samples)[8]. In addition to point mutations, deletions of *PTEN* at chromosome 10q23 are frequent in cancer (5.3% in 8,071 samples studied; **Fig. 3a**). These findings are in agreement with previous mechanistic studies demonstrating a tumor suppressor role of PTEN in acute myeloid leukemia[16], chronic myeloid leukemia (CML)[17], T cell lineage acute lymphoblastic leukemia[9,18,19] and mature B cell lymphoma[20–22]. However, point mutations in *PTEN* were not detected in any of the 694 pre-B ALL patient samples evaluated. Likewise, no *PTEN* deletions were found in the 231 pre-B ALL cases studied (**Fig. 3a**). Similarly, although oncogenic activation of the PI3K-AKT pathway in leukemia and lymphoma also occurs through activating mutations in genes encoding agonists of the PI3K-AKT pathway, pre-B ALL cases do not harbor such mutations (**Supplementary Fig. 3**). Together, these genetic data suggest that *PTEN* lesions and other mutations that lead to oncogenic activation of the PI3K-AKT pathway are not favorable in pre-B ALL and that *PTEN* may have a fundamentally different role in pre-B ALL than in other hematopoietic malignancies.

High expression levels of PTEN in patient-derived pre-B ALL cells

Consistent with these findings, our analysis of patient-derived samples showed that *PTEN* promoter regions are hypermethylated in B cell lymphomas ($n = 68$) but not in pre-B ALL samples ($n = 83$; **Fig. 3b**). Reverse-phase protein array (RPPA) measurements for 155 newly diagnosed cases of adult ALL, 22 cases of T cell lineage ALL and 11 cases of mature B cell lymphoma (the M.D. Anderson Cancer Center (MDACC) (1983–2007) cohort)[23] revealed higher PTEN protein levels in samples from individuals with pre-B ALL than in those from individuals with T cell lineage ALL or mature B cell lymphoma (**Fig. 3c**). We confirmed these findings by western blot analyses, using a panel of sorted normal human CD19$^+$ pre-B cells ($n = 3$), patient-derived pre-B ALL cells ($n = 8$) and B cell non-Hodgkin's lymphoma samples ($n = 4$) (**Fig. 3d**). The MDACC (1983–2007) cohort RPPA data set replicated results from previous work[24] that identified high expression levels of PTEN as a predictor of favorable outcome in individuals with T cell lineage ALL (**Supplementary Fig. 4**). In contrast, RPPA data for diagnostic samples from individuals with pre-B ALL showed the opposite trend, with greater-than-median expression levels of PTEN in diagnostic pre-B ALL samples being predictive of shorter relapse-free survival times (**Supplementary Fig. 4**).

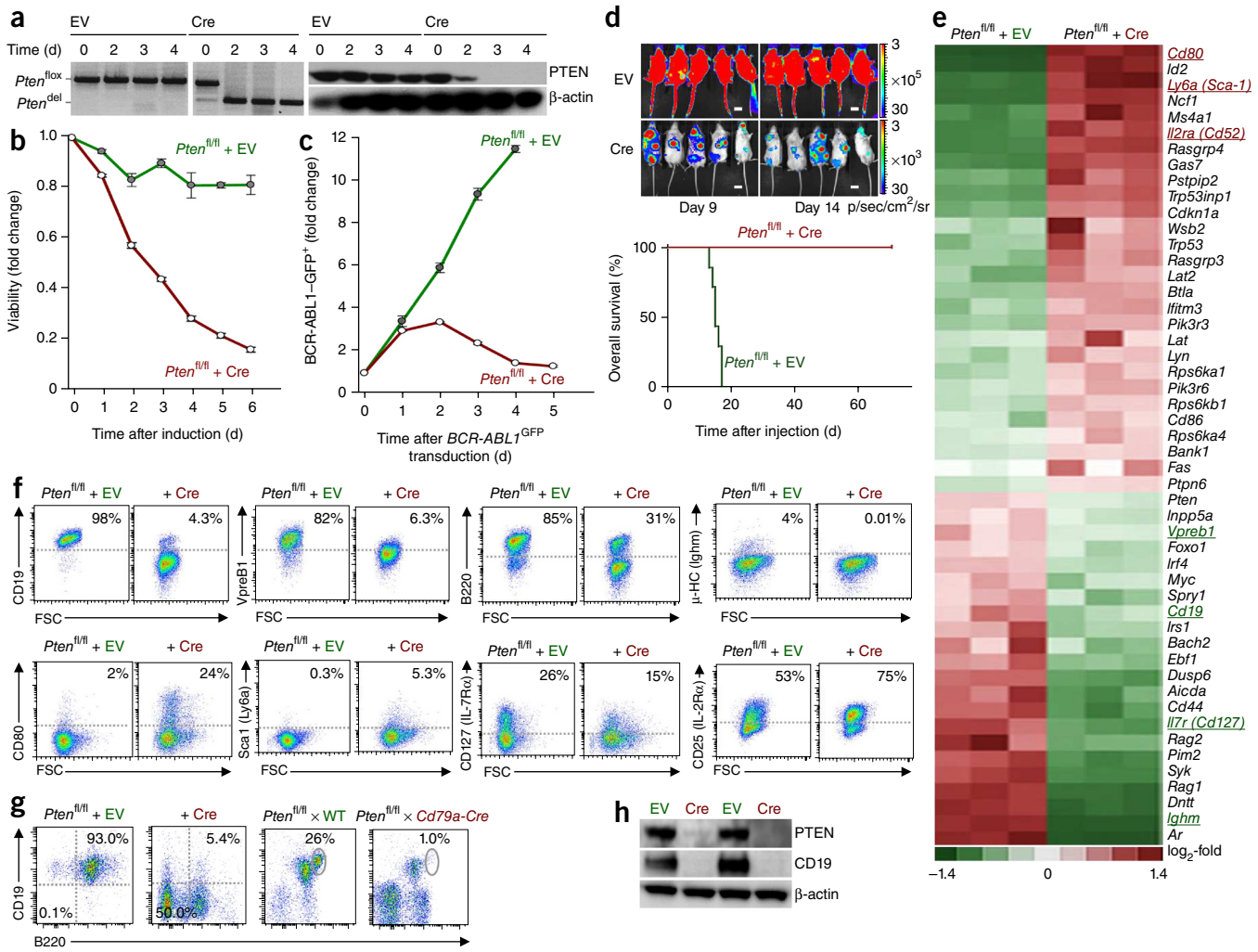

Figure 1 *Pten* is required for leukemic transformation of pre-B cells. (**a**) Representative PCR (left; $n = 3$) and western blot (right; $n = 3$) analysis for *Pten* deletion (*Pten*^{del}) after induction of *Cre* expression by Tam treatment of *BCR-ABL1*–transformed *Pten*$^{fl/fl}$ pre-B cells. β-actin was used as loading control. (**b**) Viability of *BCR-ABL1*–transformed pre-B ALL cells, as measured by flow cytometry, after tamoxifen-dependent induction of *Pten* deletion ($n = 3$). Error bars represent mean ± s.d. $P < 0.0001$; as calculated by contingency table. (**c**) The fraction of BCR-ABL1–GFP$^+$ pre-B cells, measured over time using flow cytometry. Error bars represent mean ± s.d. $P < 0.0001$; as calculated by contingency table. (**d**) Luciferase bioimaging of NOD-SCID recipient mice 9 d (left) and 14 d (right) after injection of *Pten*$^{fl/fl}$ *BCR-ABL1*–transformed pre-B ALL cells that were transduced with constructs expressing either Tam-inducible *Cre* (Cre) (bottom) or an empty vector (EV) control (top) and in which *Pten* deletion was induced 24 h before injection. Graph (bottom) shows survival analysis of the mice ($n = 7$ mice per group). Color bar for luminescent signal intensity shows photons/s/cm^2/steradian. Scale bars, 2 cm. $P = 0.0002$ was calculated by Mantel-Cox log-rank test. (**e**) Microarray gene expression analysis after 48 h of induction of *Pten* deletion in *BCR-ABL1*–transformed pre-B ALL cells. (**f**) Representative flow cytometry analysis (of $n = 3$) for cell surface expression of the indicated molecules before (*Pten*$^{fl/fl}$ + EV) and after (+ Cre) deletion of *Pten*. FSC, forward scatter. (**g**) Representative flow cytometry analysis (of $n = 3$) for the expression of the B cell markers CD19 and B220 in cells after the deletion of *Pten in vitro* (+ Cre; $n = 3$) (left) or *in vivo* (*Pten*$^{fl/fl}$ × *Cd79a-Cre*; $n = 4$) (right). (**h**) Representative western blot analysis (of $n = 4$) of *Pten*$^{fl/fl}$ *BCR-ABL1*-transformed pre-B ALL cells before (EV) and after (Cre) *Pten*$^{fl/fl}$ deletion. β-actin was used as a loading control.

Pten regulates AKT activity downstream of the pre-B cell receptor

To elucidate the mechanistic basis of *Pten* dependency in pre-B ALL, we first tested the hypothesis that loss of *Pten* results in hyperactivation of PI3K-AKT signaling and subsequent cell death. In agreement with this hypothesis, we found that inducible deletion of *Pten* in both *BCR-ABL1*– and *NRAS*^{G12D}-driven pre-B ALL cells resulted in increased phosphorylation of AKT at both Ser473 and Thr308 (**Fig. 3e**). Consistent with PTEN-dependent feedback regulation, deletion of *Pten* caused hyperactivation of PI3K-AKT signaling and downregulation of the pre-BCR, IL-7R and CD19 (**Figs. 1f–h** and **3f**), all of which mediate PI3K-AKT activation in pre-B cells. SYK is a B cell–specific tyrosine kinase that links pre-BCR signaling to PI3K activation[12–15]. To measure the contribution of individual components of the PI3K-AKT pathway in inducing toxicity, we used selective small-molecule inhibitors of the SYK (PRT06207), PI3K (BKM120) and AKT (AZD5363) kinases (**Fig. 3f**). Consistent with the toxicity induced by hyperactivation of AKT in pre-B ALL cells, pharmacological inhibition of AKT by treatment with AZD5363 greatly reduced the toxicity mediated by *Pten* deletion (**Fig. 3g** and **Supplementary Fig. 5a**). Also inhibition of SYK (using PRT06207) and PI3K (using BKM120) mitigated the toxic effects of the *Pten* deletion. Given that BCR-ABL1 and NRAS^{G12D} can activate AKT independently of SYK and PI3K, treatment of cells with the AKT inhibitor AZD5363 had the strongest protective effect in reducing cell death induced by the *Pten* deletion (**Fig. 3h** and **Supplementary Fig. 5b**).

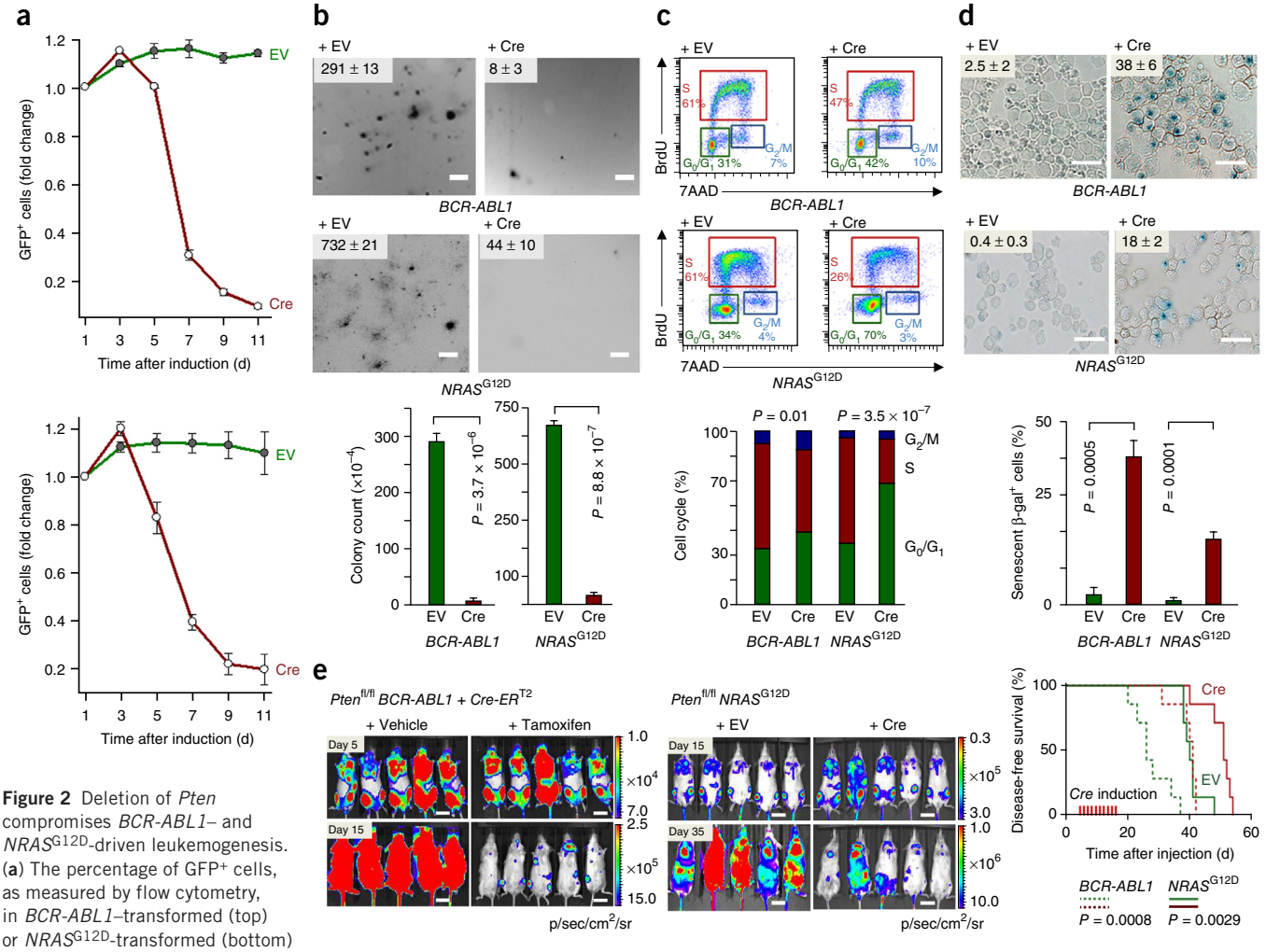

Figure 2 Deletion of *Pten* compromises *BCR-ABL1*– and *NRAS*^{G12D}-driven leukemogenesis. (**a**) The percentage of GFP$^+$ cells, as measured by flow cytometry, in *BCR-ABL1*–transformed (top) or *NRAS*^{G12D}-transformed (bottom) *Pten*$^{fl/fl}$ pre-B cells that were transduced with an inducible *Cre-ER*^{T2}–*GFP* construct or a *GFP*-expressing empty-vector control (EV) after induction of *Cre* with Tam. Error bars represent mean ± s.d. For each plot, $P < 0.0001$; as obtained by contingency table. (**b**) Representative images (top and middle) and quantification (bottom) of the colony-forming ability of *BCR-ABL1*–transformed or *NRAS*^{G12D}-transformed *Pten*$^{fl/fl}$ pre-B cells after *Pten* deletion. (**c**) Representative flow cytometry plots (top and middle) and quantification (bottom) of the induction of cell cycle arrest after 24 h of tamoxifen-induced *Pten* deletion in *BCR-ABL1*–transformed or *NRAS*^{G12D}-transformed *Pten*$^{fl/fl}$ pre-B cells. In the graph, the percentages of each phase of the cell cycle are indicated. (**d**) Representative images (top and middle) and quantification (bottom) of cellular senescence, as measured by using β-galactosidase assay, after deletion of *Pten* in *BCR-ABL1*–transformed or *NRAS*^{G12D}-transformed *Pten*$^{fl/fl}$ pre-B cells. The percentages of cells stained with blue dots are depicted on the panels. (**e**) Luciferase bioimaging of NOD-SCID recipient mice that were injected with 10^5 *Pten*$^{fl/fl}$ *BCR-ABL1*–transformed pre-B ALL cells transduced with a construct expressing *Cre-ER*^{T2} and that were treated with Tam (0.4 mg/mouse) or corn oil (vehicle) ($n = 7$ per group) (left). In a parallel experiment, NOD-SCID recipient mice were injected with 10^5 *Pten*$^{fl/fl}$ *NRAS*^{G12D}-transformed pre-B ALL cells transduced with a construct expressing *Cre-ER*^{T2} or an empty vector control (EV) (right). In the latter experiment all mice were treated with Tam (0.4 mg/mouse; $n = 7$ per group). *P* values were calculated by Mantel-Cox log-rank test. All cells were labeled with luciferase before injection. Treatments were started on day 5 after transplantation and continued for ten consecutive days. Results in **a**–**d** are representative of two independent experiments. Error bars (**a**,**b**,**d**) represent s.d. *P* values (**b**–**d**) were calculated by Student's *t*-test. Scale bars, 1 mm (**b**), 15 μm (**d**) and 2 cm (**e**).

Both alleles of *Pten* are required for survival and proliferation of pre-B ALL cells

Deletion of *PTEN* in human cancer typically affects one allele, whereas the other copy is retained[25], suggesting that cancer cells are selected for the deletion of one but not both alleles of *PTEN*. Indeed, deletion of both *Pten* alleles induces p53-dependent senescence in a model of prostate cancer, unless *Trp53* is also deleted[25]. For this reason, we studied the consequences of both heterozygous and homozygous deletion of *Pten* in mouse pre-B ALL cells (**Supplementary Fig. 6**). By comparing the cells in which either one (*Pten*$^{+/fl}$) or both (*Pten*$^{fl/fl}$) alleles of *Pten* were deleted, we found that, in contrast to solid tumor cells, both heterozygous and homozygous deletion of *Pten* affected colony formation and proliferation of pre-B ALL cells and induced cellular senescence. The deleterious effects of mono- and bi-allelic *Pten* ablation in pre-B ALL cells were indistinguishable (**Supplementary Fig. 6a**–**c**). Likewise, deletion of either both or only one allele of *Pten* compromised leukemogenesis in an *in vivo* transplant experiment, and no difference was noted between pre-B ALL cells carrying a deletion of one or both alleles of *Pten* (**Supplementary Fig. 6d**). Western blot analysis revealed that deletion of one allele of *Pten* resulted in increased phosphorylation of AKT (**Supplementary Fig. 6e**); however, this increase was less than the AKT phosphorylation observed in response to the bi-allelic deletion of *Pten*.

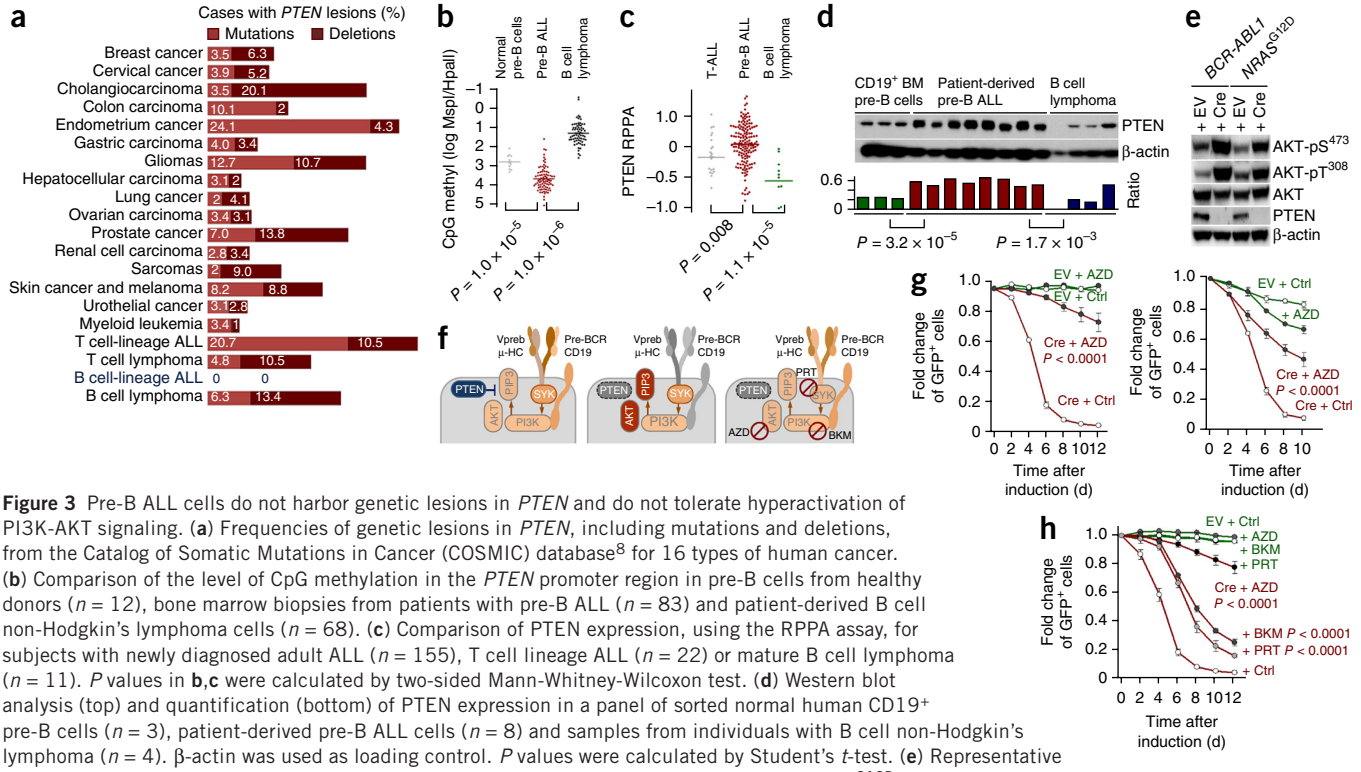

Figure 3 Pre-B ALL cells do not harbor genetic lesions in *PTEN* and do not tolerate hyperactivation of PI3K-AKT signaling. (**a**) Frequencies of genetic lesions in *PTEN*, including mutations and deletions, from the Catalog of Somatic Mutations in Cancer (COSMIC) database[8] for 16 types of human cancer. (**b**) Comparison of the level of CpG methylation in the *PTEN* promoter region in pre-B cells from healthy donors ($n = 12$), bone marrow biopsies from patients with pre-B ALL ($n = 83$) and patient-derived B cell non-Hodgkin's lymphoma cells ($n = 68$). (**c**) Comparison of PTEN expression, using the RPPA assay, for subjects with newly diagnosed adult ALL ($n = 155$), T cell lineage ALL ($n = 22$) or mature B cell lymphoma ($n = 11$). *P* values in **b**,**c** were calculated by two-sided Mann-Whitney-Wilcoxon test. (**d**) Western blot analysis (top) and quantification (bottom) of PTEN expression in a panel of sorted normal human CD19$^+$ pre-B cells ($n = 3$), patient-derived pre-B ALL cells ($n = 8$) and samples from individuals with B cell non-Hodgkin's lymphoma ($n = 4$). β-actin was used as loading control. *P* values were calculated by Student's *t*-test. (**e**) Representative western blot analysis (of $n = 3$) for AKT activation after deletion of *Pten* in *BCR-ABL1*– or *NRAS*^{G12D}-transformed pre-B ALL cells. β-actin was used as loading control. AKT-pS^{473}, phospho-Ser473 AKT; AKT-pT^{308}, phospho-Thr308 AKT. (**f**) Schematic of pre-BCR signaling and its interaction with the PI3K-AKT pathway. AZD, AZD5363; PRT, PRT06207; BKM, BKM120. (**g**) Fraction of GFP$^+$ cells, as measured by flow cytometry, after *Pten* deletion in *BCR-ABL1*–transformed (left) or *NRAS*^{G12D}-transformed (right) *Pten*$^{fl/fl}$ pre-B cells and treatment with the AKT inhibitor AZD5363 (3 μmol/liter). (**h**) Fraction of GFP$^+$ cells after *Pten*-deleted *BCR-ABL1*–transformed pre-B ALL cells in the presence or absence of AZD5363 (3 μmol/liter), the PI3K inhibitor BKM120 (1 μmol/liter) or the SYK inhibitor PRT06207 (3 μmol/liter). Throughout, for cells transduced with EV or a *Cre*-expressing vector, *P* values were calculated by contingency table, by comparing the treatment group with the untreated control group (Ctrl). All *P* values for EV-transduced cells are not significant ($P > 0.5$, not shown). Error bars represent s.d. Results are representative of three independent experiments.

AKT hyperactivation eliminates autoreactive B cells

Unlike other cell types, pre-B cells are selected for on the basis of an intermediate level of PI3K-AKT signaling strength[4–6]. Both loss- and gain-of-function mutations of *PIK3CA* and *PIK3R1* trigger negative selection of pre-B cells and cell death[4–6]. PI3K-AKT signaling is activated downstream of the pre-BCR and its co-receptor CD19 (refs. 4,5). Previous work had demonstrated that tonic activation of PI3K-AKT signaling can rescue early B cell development in the absence of a functional pre-BCR[4,5]. Here we asked whether pharmacological inhibition of PI3K-AKT signaling can rescue negative selection and cell death in response to acute activation of an autoreactive pre-BCR. To test this hypothesis, we used a reconstitution system[26] for inducible activation of pre-BCR signaling downstream of non-autoreactive (μ-HC^{NA}) or autoreactive (μ-HC^{Auto}) μ–heavy chains or an empty-vector control (EV; **Fig. 4a**). Tamoxifen (Tam)-induced assembly of the proximal BCR signalosome in the presence of EV or μ-HC^{NA} had no effect on the viability of *BCR-ABL1*–expressing pre-B ALL cells (**Fig. 4b** and **Supplementary Fig. 7a**). However, inducible activation of signaling from an autoreactive pre-BCR (μ-HC^{Auto}) caused rapid cell death, which could be rescued by small-molecule inhibition of SYK (using PRT06207) and AKT (using AZD5363) kinase activity (**Fig. 4b** and **Supplementary Fig. 7a**). Activation of signaling from an autoreactive μ-HC (μ-HC^{Auto}) and induction of cell death involved phosphorylation of SYK and AKT, whereas activation of pre-BCR signaling downstream of μ-HC^{NA} and EV had no effect on phosphorylation levels of SYK and AKT (**Fig. 4c**). Treatment with the SYK and AKT inhibitors rescued toxicity and demonstrated that hyperactivation of SYK and AKT downstream of signaling through an autoreactive pre-BCR was required to induce cell toxicity by engaging a negative selection checkpoint (**Fig. 4b**). We conclude that hyperactivation of PI3K-AKT signaling after deletion of *Pten* is functionally equivalent to hyperactivation of PI3K-AKT downstream of signaling through an autoreactive pre-BCR via SYK. Both events trigger a deletional checkpoint for the removal of autoreactive B cell clones.

To demonstrate the toxic effects of SYK and AKT hyperactivation in a genetic experiment, we transduced pre-B ALL cells with constitutively active (CA) forms of SYK (SYK^{CA}) and AKT (AKT^{CA}) and measured pre-B ALL cell viability in the presence or absence of the Syk, PI3K and AKT inhibitors. As predicted, SYK^{CA} rapidly induced cell death in pre-B ALL cells, which could be almost completely rescued by inhibition of SYK, PI3K and AKT kinase activity (**Fig. 4d** and **Supplementary Fig. 7b**). Likewise, hyperactivation of AKT (AKT^{CA}) was toxic in pre-B ALL cells, and toxicity was reduced by treatment with AKT kinase inhibitor AZD5363 (**Fig. 4e** and **Supplementary Fig. 7c**). Collectively, these findings suggest that hyperactivation of PI3K-AKT signaling engages a deletional checkpoint for the removal of autoreactive B cells.

B cell–specific expression and activity of PTEN

To test the basic premise of a checkpoint for the elimination of autoreactive pre-B cells, we reprogrammed pre-B ALL cells into myeloid lineage cells using an inducible CCAAT–enhancer-binding

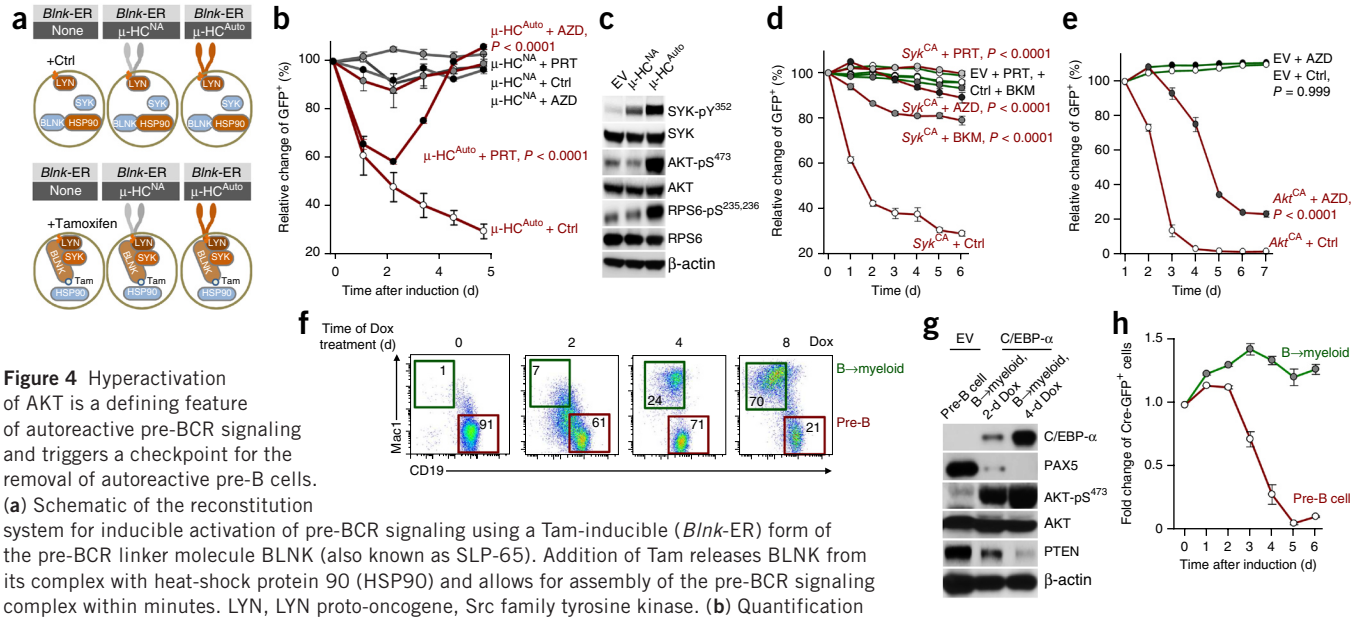

Figure 4 Hyperactivation of AKT is a defining feature of autoreactive pre-BCR signaling and triggers a checkpoint for the removal of autoreactive pre-B cells. (**a**) Schematic of the reconstitution system for inducible activation of pre-BCR signaling using a Tam-inducible (*Blnk*-ER) form of the pre-BCR linker molecule BLNK (also known as SLP-65). Addition of Tam releases BLNK from its complex with heat-shock protein 90 (HSP90) and allows for assembly of the pre-BCR signaling complex within minutes. LYN, LYN proto-oncogene, Src family tyrosine kinase. (**b**) Quantification of GFP$^+$ cells, relative to that in EV-transduced cells, after activation of pre-B cell signaling in *BCR-ABL1*–transformed pre-B ALL cells with 2 d of pre-treatment with inhibitors of SYK (PRT, 3 μmol/liter) or AKT (AZD, 3 μmol/liter). For each curve, the *P* value was calculated by contingency table, by comparing treatment groups with untreated control group (Ctrl). *P* values for μ-HC^{NA}–transduced cells were not significant (>0.5, not shown). (**c**) Representative western blot analysis (of $n = 2$) for the phosphorylation of SYK, AKT and the ribosomal protein RPS6 5 min after addition of tamoxifen. (**d**) Relative changes in the percentages of GFP$^+$ cells after transduction of pre-B ALL cells with a construct that expresses a GFP-tagged constitutively active SYK (*Syk*^{CA}; *Syk*^{Y348E,Y352E}) or empty vector (EV) control in the presence of vehicle or inhibitors of AKT (AZD, 3 μmol/liter), PI3K (BKM, 1 μmol/liter) and SYK (PRT, 3 μmol/liter). (**e**) Relative changes in the percentages of GFP$^+$ cells after transduction of pre-B ALL cells with a GFP-tagged retroviral vector encoding myristoylated AKT (*Akt*^{CA}) or GFP (EV) control in the presence or absence of the AKT inhibitor (AZD, 3 μmol/liter). (**f**) Representative flow cytometry analysis (of $n = 3$) for B→myeloid reprogramming of *BCR-ABL1*–transformed *Pten*$^{fl/fl}$ pre-B ALL (CD19$^+$Mac1$^-$) to myeloid lineage (CD19$^-$Mac1$^+$) cells after induction of C/EBP-α by doxycycline (Dox) treatment. (**g**) Representative western blot analysis (of $n = 2$) for the expression of C/EBP-α, the B cell lineage–specific transcription factor PAX5, total and phospho-Ser473 AKT, and PTEN in B-lineage and B→myeloid reprogrammed cells. (**h**) Changes in the frequency of GFP$^+$ cells in B→myeloid (CD19$^-$Mac1$^+$) and pre-B cells (CD19$^+$Mac1$^-$) after induction of *Cre-GFP* by Tam treatment. $P < 0.0001$ was calculated using contingency table. All results presented in this figure are representative of two independent experiments with triplicates. Error bars (**b**,**d**,**e**,**h**) represent mean ± s.d. For curves in **b**,**d**,**e**, *P* values were calculated by contingency table comparing treatment groups with the respective untreated control group (Ctrl).

protein alpha (C/EBP-α) vector system[27]. To this end, we engineered *Pten*$^{fl/fl}$ pre-B ALL cells with a doxycycline-inducible vector system for expression of the myeloid transcription factor C/EBP-α, which results in B→myeloid lineage conversion (**Fig. 4f–h**). Inducible expression of C/EBP-α in pre-B ALL cells not only downregulated PAX5, a transcription factor that determines B cell lineage identity, but also resulted in downregulation of PTEN levels, demonstrating that PTEN expression levels depend on B cell lineage identity (**Fig. 4g**). C/EBP-α–mediated myeloid lineage conversion also resulted in a 45-fold increase in phosphorylation of Ser473 in AKT, as compared to that in the EV-transduced cells, which mirrors transcriptional repression of PTEN in myeloid cells (**Fig. 4g**). These findings are consistent with the notion that myeloid cells, unlike B lineage cells, are permissive to the loss of PTEN function and hyperactivation of AKT signaling.

To test whether B→myeloid lineage conversion erases dependency on PTEN-mediated negative regulation of AKT activity, *Pten*$^{fl/fl}$ pre-B ALL cells carrying inducible C/EBP-α or empty-vector controls (EV) were also induced to express Cre (**Fig. 4h**). Inducible deletion of *Pten* resulted in a rapid elimination of B cell–lineage ALL cells (CD19$^+$Mac1$^-$) as in previous experiments (**Fig. 1c–f** and **Supplementary Fig. 1**). By contrast, deletion of *Pten* in B→myeloid–reprogrammed cells (CD19$^-$Mac1$^+$) resulted in a slight increase in the frequency of Cre-GFP$^+$ cells, reflecting a relative survival advantage for *Pten* deletion in myeloid cells (**Fig. 4h**). These findings are consistent with a previous study[17] that identified PTEN as a tumor suppressor in *BCR-ABL1*–transformed myeloid leukemia and reinforce the notion that normal pre-B and pre-B ALL cells are uniquely dependent on negative regulation of AKT by PTEN.

The deleterious effects of *Pten* deletion in pre-B ALL are linked to B cell lineage identity

Pre-B (*Ph*$^+$ ALL) and CML are both driven by the oncogenic BCR-ABL1 tyrosine kinase but markedly differ with respect to PTEN expression levels (**Fig. 5a**,**b**). PTEN protein levels were high in *BCR-ABL1*–driven mouse pre-B ALL cells and in patient-derived *Ph*$^+$ ALL cells ($n = 5$) but barely detectable in mouse CML-like and in patient-derived CML cells ($n = 5$; **Fig. 5a**,**b**). This difference is consistent with regulation of *Pten* levels during B→myeloid reprogramming (**Fig. 4g**). Although pre-B cells are subject to a deletional checkpoint for the removal of autoreactive clones, this is not the case for other cell types (including myeloid cells). Similarly, deletion of *Pten* in normal myeloid progenitor cells showed no effects but caused toxicity in normal pre-B cells (**Fig. 5c**). Moreover, Cre-mediated *Pten* deletion had no deleterious effects in *BCR-ABL1* myeloid lineage CML but caused cell death in *BCR-ABL1*–transformed pre-B ALL cells (**Fig. 5d**). Induction of cell death after *Pten* deletion in pre-B ALL cells was paralleled by accumulation of the ARF, p53 and p21 cell cycle checkpoint molecules. In contrast, *Pten* deletion in myeloid leukemia cells induced neither activation of checkpoint molecules nor cell death

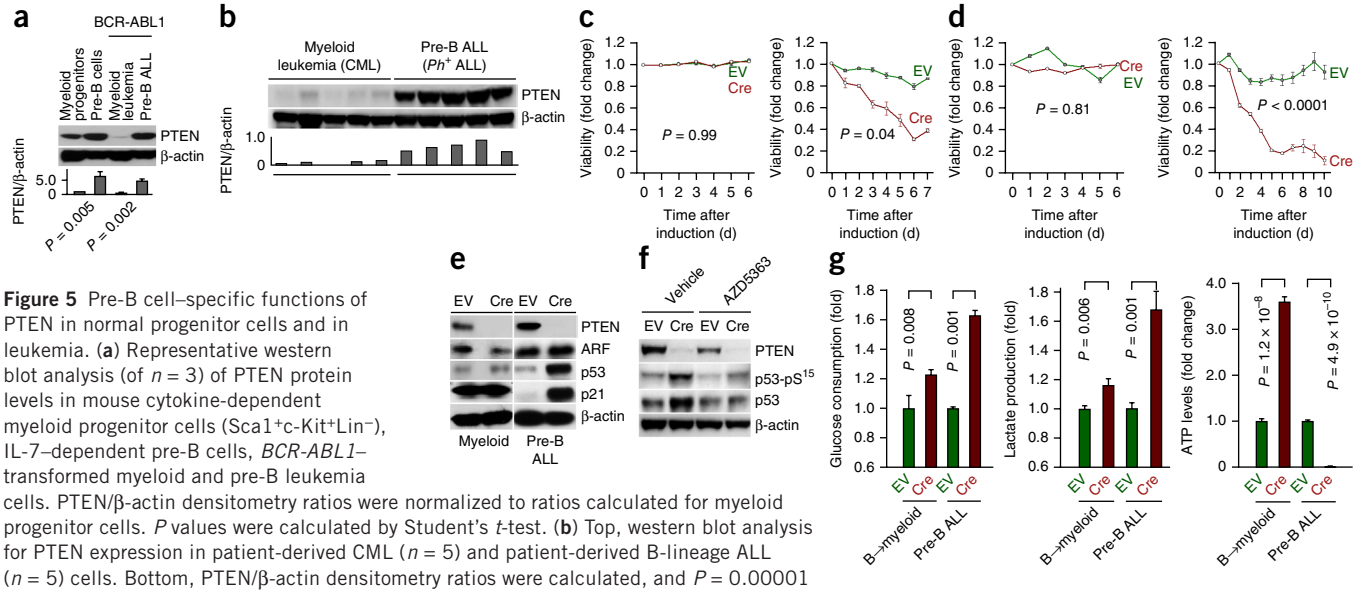

Figure 5 Pre-B cell–specific functions of PTEN in normal progenitor cells and in leukemia. (**a**) Representative western blot analysis (of $n = 3$) of PTEN protein levels in mouse cytokine-dependent myeloid progenitor cells (Sca1$^+$c-Kit$^+$Lin$^-$), IL-7–dependent pre-B cells, *BCR-ABL1*–transformed myeloid and pre-B leukemia cells. PTEN/β-actin densitometry ratios were normalized to ratios calculated for myeloid progenitor cells. *P* values were calculated by Student's *t*-test. (**b**) Top, western blot analysis for PTEN expression in patient-derived CML ($n = 5$) and patient-derived B-lineage ALL ($n = 5$) cells. Bottom, PTEN/β-actin densitometry ratios were calculated, and $P = 0.00001$ was calculated by Student's *t*-test. (**c**,**d**) The percentages of viable cells were measured after Cre-induced *Pten* deletion in myeloid progenitor cells (**c**, left) and pre-B cells (**c**, right) and their *BCR-ABL1*–transformed counterpart CML-like (**d**, left) and pre-B ALL (**d**, right) cells ($n = 2$). *P* values were calculated using contingency tables. (**e**) Representative western blot analysis (of $n = 2$) for expression of cell cycle–checkpoint molecules ARF, p53 and p21 after deletion of *Pten* in *BCR-ABL1*–transformed myeloid leukemia and pre-B ALL cells. (**f**) Representative western blot analysis (of $n = 3$) for total p53 and p53 (phospho-Ser15) after 48 h of Cre-induced *Pten* deletion in *BCR-ABL1*–transformed pre-B ALL in the presence of the AKT inhibitor (AZD, 3 μmol/liter) or vehicle. (**g**) Glucose consumption, lactate production and ATP levels on day 2 following induction of *Cre* in *Pten*$^{fl/fl}$ *BCR-ABL1*–transformed pre-B ALL or myeloid reprogrammed cells. Values obtained were normalized to the number of viable cells and are shown as average relative levels. *P* values were calculated by Student's *t*-test. β-actin was used as loading control (**a**,**b**,**e**,**f**). Error bars (**a**,**c**,**d**,**g**) represent mean ± s.d.

(**Fig. 5d**,**e**). Consistent with its function as a regulator of an autoimmunity checkpoint, these findings suggest that PTEN is specifically required for the survival of normal and transformed pre-B cells and is dispensable in myeloid cells. Activation of p53 after deletion of *Pten* involved increased p53 phosphorylation at Ser15, which increases p53 stability and its half-life (**Fig. 5f**). Notably, both Ser15-phosphorylation and accumulation of p53 were reversed by AKT inhibition (by AZD5363 treatment), indicating that activation of p53 in response to *Pten* deletion is caused by AKT hyperactivation (**Fig. 5f**).

AKT hyperactivity exacerbates glucose and energy depletion

AKT promotes glycolysis and the use of cellular ATP for translation, cell growth and proliferation through activation of mechanistic target of rapamycin complex I (mTORC1)[28,29]. We studied the metabolic consequences of *Pten* deletion on glycolysis and energy supply after inhibiting mTORC1 activity by treatment with rapamycin. As expected, inducible deletion of *Pten* resulted in an increase in glycolysis, as measured by increased glucose consumption and increased production of lactate (**Supplementary Fig. 8**). These effects were reversed by rapamycin treatment, indicating that the increased levels of glycolysis observed after *Pten* deletion were caused by mTORC1 activation. Consistent with increased energy-inefficient glycolysis, inducible deletion of *Pten* in pre-B ALL cells reduced ATP levels, which were restored by rapamycin treatment (**Supplementary Fig. 8**). These metabolic effects of *Pten* deletion were specific for B lymphoid cells. B→myeloid reprogramming of pre-B ALL cells using inducible expression of C/EBP-α (**Fig. 4f–h**) revealed that ablation of *Pten* had divergent outcomes in B lymphoid and B→myeloid–reprogrammed leukemia cells. Although loss of *Pten* moderately increased glycolysis in myeloid cells, resulting in a substantial net gain of cellular ATP levels, glycolytic activity was excessively increased in B lymphoid cells, which resulted in depletion of glucose reserves and in near-exhaustion of cellular ATP levels (**Fig. 5g**). Taken together, these findings indicate that deletion of *Pten* in pre-B ALL cells caused profound metabolic distress in conjunction with strong activation of p53 checkpoint activation in pre-B ALL cells. It should be noted that we tested alternative mechanisms of toxicity related to *Pten* deletion, including dephosphorylation of signal transducer and activator of transcription 5 (STAT5) and accumulation of cellular reactive-oxygen species (ROS). Unlike metabolic stress and p53-mediated cell death, loss of STAT5 phosphorylation and increased ROS levels were only observed in *BCR-ABL1*–transformed ALL cells and could not be mechanistically validated in other ALL subtypes (data not shown).

Validation of PTEN as a therapeutic target in patient-derived pre-B ALL cells

Despite the well-characterized function of PTEN as a tumor suppressor, to test whether PTEN represents a therapeutic target in human pre-B ALL, we used patient-derived pre-B ALL cells in which either of two distinct shRNAs specific for *PTEN* or a scrambled control shRNA were delivered using a lentivirus. Expression of the *PTEN*-specific shRNA hairpins reduced PTEN protein levels by twofold to fourfold as compared to expression of the nontargeting (scrambled) control, as determined by western blot analysis (**Fig. 6a**). shRNA-mediated knockdown of *PTEN* in three human myeloid lineage CML cell lines did not affect cell viability, as compared to cells expressing the control shRNA (**Fig. 6b** and **Supplementary Fig. 9**). In contrast, *PTEN* knockdown induced cell death in cells from four individuals with pre-B ALL who harbored the *BCR-ABL1* (subjects LAX2 and ICN1), *TCF3-PBX1* (subject ICN12) or *KRAS*^{G12V} (subject LAX7R) oncogenes (**Fig. 6b** and **Supplementary Fig. 9**). We conclude that PTEN is essential for the survival of human pre-B ALL cells, thus validating PTEN as a potential therapeutic target in human pre-B ALL.

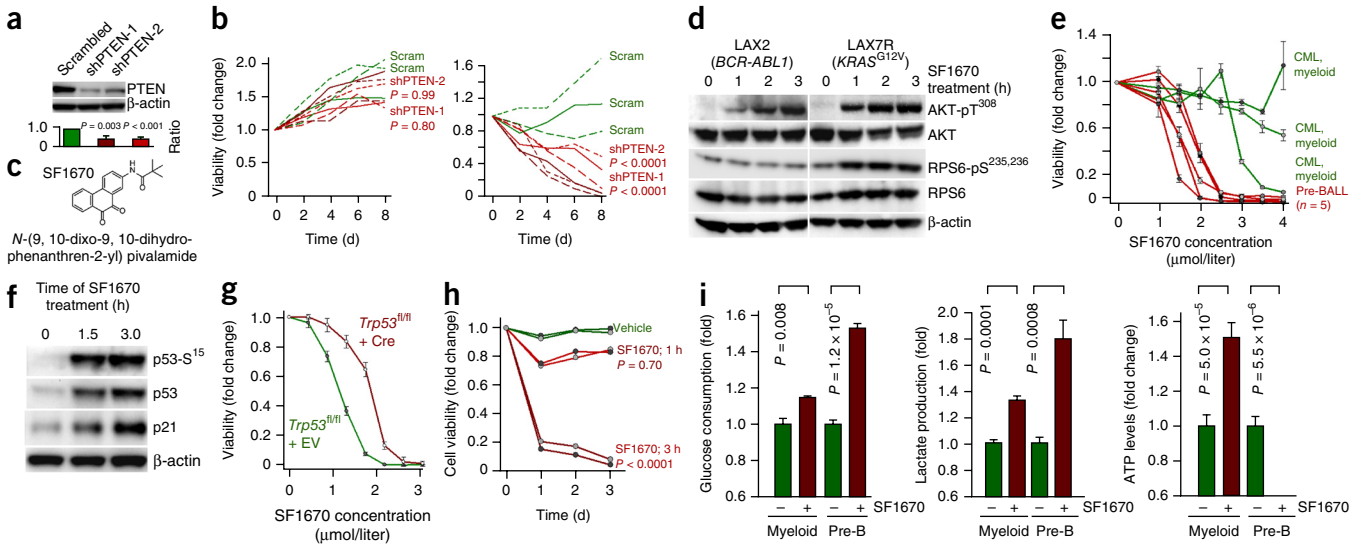

Figure 6 A small-molecule inhibitor of PTEN is specifically toxic in pre-B ALL. (**a**) Representative western blots (of $n = 3$) (top) and quantification (bottom) after *PTEN* knockdown with either of two PTEN-specific shRNAs (shPTEN-1 and shPTEN-2) in pre-B ALL xenografts and CML cell lines. β-actin was used as a loading control. *P* values were calculated by Student's *t*-test comparing PTEN levels in cells expressing each *PTEN*-specific shRNA to that from cells expressing the scrambled shRNA. (**b**) Viability of three CML cell lines (KYO-1, solid line; KU812, short-dashed line; JURL-MK1, long-dashed line) (left) and three patient-derived pre-B ALL xenografts (LAX7R, solid line; LAX2, short-dashed line; ICN12, long-dashed line) (right) after transduction with either of two shRNAs specific for *PTEN* or a scrambled (Scram) sequence. *P* values were calculated using contingency tables comparing average viability of cells for each shRNA versus scrambled control. (**c**) Chemical structure of the PTEN inhibitor SF1670. (**d**) Representative western blot analysis (of $n = 4$) for induction of the AKT signaling pathway after SF1670 (10 μmol/liter) treatment of cells from two individuals with pre-B ALL. β-actin was used as loading control. (**e**) Viability of human cells from individuals with pre-B ALL ($n = 5$, red) or CML ($n = 3$, green) after SF1670 treatment. Error bars represent mean ± s.d. $P < 0.0001$ was calculated using contingency table comparing viability of cells from individuals with Pre-B ALL versus those with CML. (**f**) Representative western blot analysis (of $n = 3$) for p21, p53 and p53 (phospho-Ser15) on pre-B ALL cells treated with SF1670 (10 μmol/liter). β-actin was used as loading control. (**g**) Viability of *BCR-ABL1*-transformed pre-B ALL cells with or without *Trp53* deletion after SF1670 treatment. Error bars represent mean ± s.d. $P < 0.001$ was calculated by contingency table. (**h**) Viability of cells from two individuals with pre-B ALL after treatment for 1 h or 3 h with SF1670 (10 μmol/liter) for three consecutive days. *P* values were calculated by contingency table comparing average cell viability after each treatment to those of vehicle-treated cells. The results are representative of three independent experiments. (**i**) Glucose consumption, lactate production and ATP levels in a CML cell line (KYO-1) and in a patient-derived pre-B ALL cells (LAX7R) after a 24-h treatment with SF1670 (2.5 μmol/liter). Values obtained were normalized to the number of viable cells and are shown as average relative levels. *P* values were calculated by Student's *t*-test. Error bars represent mean ± s.d.

Preclinical evaluation of PTEN inhibitor in pre-B ALL treatment

To test potential therapeutic usefulness of the pharmacological inhibition of PTEN, we studied the effects of a small-molecule inhibitor of PTEN, SF1670 (refs. 30,31), in human pre-B ALL cells (**Fig. 6c**). Biochemical validation of SF1670 activity revealed that treatment with this PTEN inhibitor induced activation of AKT signaling in cells from individuals with pre-B ALL who carried the *BCR-ABL1* or *KRAS*^{G12V} oncogenes within 1 h of treatment (**Fig. 6d**). SF1670 treatment strongly and selectively induced cell death in pre-B ALL cells at similar concentrations that were previously used to stimulate neutrophils *in vivo*[31] (concentration required for stimulation of 50% of cells (IC_{50}) = 1.2 μmol/liter; **Fig. 6e** and **Supplementary Fig. 10a**). In addition, treatment with SF1670 shows a similar B cell lineage–specific effect to that observed using genetic approaches (i.e., deletion of *Pten* and shRNA-mediated knockdown of *PTEN*), as myeloid CML cells were either not affected by SF1670 treatment or affected only at higher concentrations (**Fig. 6e**). In addition, treatment of human pre-B ALL cells with SF1670 phenocopied the effects of a genetic deletion of *Pten*$^{fl/fl}$ in pre-B ALL cells. Of note, the acute deletion of *Pten* in *Pten*$^{fl/fl}$ pre-B ALL cells resulted in phosphorylation (Ser15) and activation of p53 (**Fig. 5f**). Similarly, small-molecule inhibition of PTEN resulted in rapid activation of the p53 and p21 checkpoint molecules and in p53 phosphorylation at Ser15 (**Fig. 6f**). To test whether p53 checkpoint activation represents an important aspect of toxicity in pre-B ALL cells that results from acute PTEN inhibition, we transduced *Trp53*$^{fl/fl}$ *BCR-ABL1*–transformed pre-B cells with a *Cre*-expressing or an empty-vector (EV) construct. Notably, *Trp53* deletion caused a substantial shift in the dose-response curves of cells treated with SF1670. (**Fig. 6g**). Although Cre-mediated deletion of *Pten* resulted in the rapid loss of cell surface expression of CD19 and the pre-BCR (VpreB) (**Fig. 1f** and **Supplementary Fig. 10b**), we observed the same effects in human pre-B ALL cells that were treated for 2 d with SF1670 (**Supplementary Fig. 10b**). Because prolonged systemic inhibition of PTEN would presumably raise safety concerns owing to its role as a tumor suppressor in a wide range of cell types[8,18], we tested the effects of short, transient inhibition of PTEN using SF1670 treatment. A single exposure to SF1670 for 3 h (and subsequent washout of SF1670) induced AKT hyperactivation and caused significant cell death in pre-B ALL cells ($P < 0.001$; **Fig. 6h**).

Small-molecule inhibition of PTEN also recapitulated metabolic features of the genetic deletion of *Pten* (**Fig. 6i**). Although SF1670 treatment resulted in a moderate stimulation of glycolysis (glucose consumption and lactate production) in CML cells, stimulation of glycolytic responses was much stronger in B lymphoid ALL cells (**Fig. 5g**). However, SF1670 treatment resulted in a net increase in cellular ATP in myeloid CML cells but a near-complete depletion of energy reserves in patient-derived pre-B ALL cells. Thus, SF1670 treatment induced pre-B cell–specific depletion of ATP and energy crisis, which recapitulated the measurements we observed in response to Cre-mediated deletion of *Pten* in myeloid leukemia and pre-B ALL cells (**Fig. 5g**).

DISCUSSION

Unlike other cell types, pre-B cells are under intense selective pressure and have to pass a central B cell tolerance checkpoint that removes autoreactive clones[2]. The vast majority of newly generated pre-B cells express an autoreactive immunoglobulin μ–heavy chain, which results in strong pre-B cell receptor signaling, and are eliminated at this checkpoint[2,3]. Humans carrying germline mutations that result in hyperactive PI3K-AKT signaling have profound B cell lymphopenia[6], presumably because almost all newly generated pre-B cells are subject to negative selection owing to hyperactive PI3K-AKT signaling. Recent work from our group demonstrated that central B cell tolerance checkpoints are fully functional in human pre-B ALL cells, despite their malignant transformation[32,33]. Here we demonstrated that PTEN represents a critical gatekeeper of this checkpoint. Despite its tumor suppressor function in all major subtypes of cancer, PTEN is required to prevent indiscriminate checkpoint activation. Reflecting the unique function of PTEN in central B cell tolerance, pre-B ALL was the only subtype of human cancer that we found to be exempt from *PTEN* lesions (**Fig. 3a**). Previous work demonstrated that pre-B cells need a minimum level of PI3K-AKT signaling to survive[5] and that targeting of this pathway is potentially useful in the treatment of human pre-B ALL[34]. However, here we propose that acute inhibition of PTEN or direct pharmacological hyperactivation of PI3K-AKT signaling may represent a strategy to trigger central B cell tolerance checkpoints and thereby overcome conventional drug resistance in human pre-B ALL.

METHODS

Methods and any associated references are available in the online version of the paper.

Accession codes. Gene Expression Omnibus: the array data has been deposited with accession code GSE34829.

Note: Any Supplementary Information and Source Data files are available in the online version of the paper.

ACKNOWLEDGMENTS

We would like to thank L.M. Staudt (National Cancer Institute), D.A. Fruman (University of California, Irvine), T. Kurosaki (World Premier International (WPI) Immunology Frontier Research Center), S. Li (Dana-Farber Cancer Institute) and A. Weiss (University of California, San Francisco) for comments and critical discussion of this study. This work is supported by the US National Institutes of Health (NIH) and the National Cancer Institute through grants R01CA137060 (M.M.), R01CA139032 (M.M.), R01CA157644 (M.M.), R01CA169458 (M.M.) and R01CA172558 (M.M.), the William Lawrence and Blanche Hughes Foundation (M.M.), the California Institute for Regenerative Medicine (CIRM; grant TR2-01816; M.M.) and Bloodwise (M.M.). T.G.G. is the recipient of a Research Scholar Award from the American Cancer Society (award RSG-12-257-01-TBE), an Established Investigator Award from the Melanoma Research Alliance (award 20120279), and is supported by NIH–National Center for Advancing Translational Science (NCATS) UCLA CTSI grant UL1TR000124. M.M. is a Scholar of the Leukemia and Lymphoma Society and a Senior Investigator of the Wellcome Trust.

AUTHOR CONTRIBUTIONS

S.S. and M.M. designed experiments and interpreted data; M.M. conceived the study, obtained funding, coordinated collaborations and wrote the paper; S.S., L.N.C., M.B., V.C., K.N.C. and H.G. performed experiments and analyzed data; Y.H.Q., A.M. and S.M.K. provided and characterized patient samples or cell lines and clinical outcome data; H.W. provided important reagents and mouse samples; M.D.v.M., T.E., A.H., G.C., S.M.K., T.G.G. and H.J. provided conceptual input to the design of the study.

COMPETING FINANCIAL INTERESTS

The authors declare no competing financial interests.

1. Osmond, D.G. Proliferation kinetics and the lifespan of B cells in central and peripheral lymphoid organs. *Curr. Opin. Immunol.* **3**, 179–185 (1991).
2. Wardemann, H. *et al.* Predominant autoantibody production by early human B cell precursors. *Science* **301**, 1374–1377 (2003).
3. Keenan, R.A. *et al.* Censoring of autoreactive B cell development by the pre-B cell receptor. *Science* **321**, 696–699 (2008).
4. Srinivasan, L. *et al.* PI3 kinase signals BCR-dependent mature B cell survival. *Cell* **139**, 573–586 (2009).
5. Ramadani, F. *et al.* The PI3K isoforms p110-α and p110-δ are essential for pre-B cell receptor signaling and B cell development. *Sci. Signal.* **3**, ra60 (2010).
6. Deau, M.C. *et al.* A human immunodeficiency caused by mutations in the *PIK3R1* gene. *J. Clin. Invest.* **124**, 3923–3928 (2014).
7. Vivanco, I. & Sawyers, C.L. The phosphatidylinositol 3-kinase–AKT pathway in human cancer. *Nat. Rev. Cancer* **2**, 489–501 (2002).
8. Futreal, P.A. *et al.* A census of human cancer genes. *Nat. Rev. Cancer* **4**, 177–183 (2004).
9. Gutierrez, A. *et al.* High frequency of *PTEN*, *PI3K* and *AKT* abnormalities in T cell acute lymphoblastic leukemia. *Blood* **114**, 647–650 (2009).
10. Lesche, R. *et al.* Cre-*loxP*–mediated inactivation of the murine *Pten* tumor suppressor gene. *Genesis* **32**, 148–149 (2002).
11. Zhang, J. *et al.* Key pathways are frequently mutated in high-risk childhood acute lymphoblastic leukemia: a report from the Children's Oncology Group. *Blood* **118**, 3080–3087 (2011).
12. Guo, B., Kato, R.M., Garcia-Lloret, M., Wahl, M.I. & Rawlings, D.J. Engagement of the human pre-B cell receptor generates a lipid raft–dependent calcium signaling complex. *Immunity* **13**, 243–253 (2000).
13. Okada, T., Maeda, A., Iwamatsu, A., Gotoh, K. & Kurosaki, T. BCAP: the tyrosine kinase substrate that connects B cell receptor to phosphoinositide 3-kinase activation. *Immunity* **13**, 817–827 (2000).
14. Anzelon, A.N., Wu, H. & Rickert, R.C. *Pten* inactivation alters peripheral B lymphocyte fate and reconstitutes CD19 function. *Nat. Immunol.* **4**, 287–294 (2003).
15. Aiba, Y., Kameyama, M., Yamazaki, T., Tedder, T.F. & Kurosaki, T. Regulation of B cell development by BCAP and CD19 through their binding to phosphoinositide 3-kinase. *Blood* **111**, 1497–1503 (2008).
16. Tesio, M. *et al. Pten* loss in the bone marrow leads to G-CSF–mediated HSC mobilization. *J. Exp. Med.* **210**, 2337–2349 (2013).
17. Peng, C. *et al. PTEN* is a tumor suppressor in CML stem cells and in BCR-ABL–induced leukemias in mice. *Blood* **115**, 626–635 (2010).
18. Li, J. *et al. PTEN*, a putative protein tyrosine phosphatase gene mutated in human brain, breast and prostate cancer. *Science* **275**, 1943–1947 (1997).
19. Gutierrez, A. *et al. Pten* mediates *Myc* oncogene dependence in a conditional zebrafish model of T cell acute lymphoblastic leukemia. *J. Exp. Med.* **208**, 1595–1603 (2011).
20. Lenz, G. *et al.* Molecular subtypes of diffuse large B cell lymphoma arise by distinct genetic pathways. *Proc. Natl. Acad. Sci. USA* **105**, 13520–13525 (2008).
21. Miletic, A.V. *et al.* Coordinate suppression of B cell lymphoma by PTEN and SHIP phosphatases. *J. Exp. Med.* **207**, 2407–2420 (2010).
22. Pfeifer, M. *et al. PTEN* loss defines a PI3K-AKT pathway–dependent germinal center subtype of diffuse large B cell lymphoma. *Proc. Natl. Acad. Sci. USA* **110**, 12420–12425 (2013).
23. Tibes, R. *et al.* Reverse-phase protein array: validation of a novel proteomic technology and utility for analysis of primary leukemia specimens and hematopoietic stem cells. *Mol. Cancer Ther.* **5**, 2512–2521 (2006).
24. Roman-Gomez, J. *et al.* Lack of CpG island methylator phenotype defines a clinical subtype of T cell acute lymphoblastic leukemia associated with good prognosis. *J. Clin. Oncol.* **23**, 7043–7049 (2005).
25. Chen, Z. *et al.* Crucial role of p53-dependent cellular senescence in suppression of *Pten*-deficient tumorigenesis. *Nature* **436**, 725–730 (2005).
26. Köhler, F. *et al.* Autoreactive B cell receptors mimic autonomous pre-B cell receptor signaling and induce proliferation of early B cells. *Immunity* **29**, 912–921 (2008).
27. Xie, H., Ye, M., Feng, R. & Graf, T. Stepwise reprogramming of B cells into macrophages. *Cell* **117**, 663–676 (2004).
28. Shackelford, D.B. *et al.* mTOR and HIF-1α–mediated tumor metabolism in an *LKB1* mouse model of Peutz-Jeghers syndrome. *Proc. Natl. Acad. Sci. USA* **106**, 11137–11142 (2009).
29. Düvel, K. *et al.* Activation of a metabolic gene regulatory network downstream of mTOR complex 1. *Mol. Cell* **39**, 171–183 (2010).
30. Rosivatz, E. *et al.* A small-molecule inhibitor for phosphatase and tensin homolog deleted on chromosome 10 (PTEN). *ACS Chem. Biol.* **1**, 780–790 (2006).
31. Li, Y. *et al.* Pretreatment with phosphatase and tensin homolog deleted on chromosome 10 (PTEN) inhibitor SF1670 augments the efficacy of granulocyte transfusion in a clinically relevant mouse model. *Blood* **117**, 6702–6713 (2011).
32. Chen, Z. *et al.* Signaling thresholds and negative B cell selection in acute lymphoblastic leukemia. *Nature* **521**, 357–361 (2015).
33. Shojaee, S. *et al.* Erk negative feedback control enables pre B cell transformation and represents a therapeutic target in acute lymphoblastic leukemia. *Cancer Cell* **28**, 114–128 (2015).
34. Kharas, M.G. *et al.* Ablation of PI3K blocks *BCR-ABL* leukemogenesis in mice, and a dual PI3K-mTOR inhibitor prevents expansion of human BCR-ABL$^+$ leukemia cells. *J. Clin. Invest.* **118**, 3038–3050 (2008).

ONLINE METHODS

Patient samples, human cells and cell lines. We obtained primary patient samples (**Supplementary Table 1**) in compliance with the Institutional Review Board of the University of California, San Francisco. Human leukemia cells were maintained in Minimum Essential Medium alpha (MEM-α, Invitrogen, Carlsbad, CA) supplemented with GlutaMAX, 20% FBS, 100 IU/ml penicillin and 100 µg/ml streptomycin and incubated at 37 °C in a humidified incubator with 5% CO_2. We obtained informed consent from all participants. Primary human ALL cells (patient samples) were cultured on irradiated OP9 stromal cells (American Type Culture Collection, Manassas, VA) in the same medium as described above.

Retroviral transduction. A complete list of vectors used in this study is provided in **Supplementary Table 2**. Transfections of the murine stem cell virus (MSCV)-based retroviral constructs were performed using Lipofectamine 2000 (Invitrogen, Carlsbad, CA) with Opti-MEM medium (Invitrogen). Retroviral supernatant was produced by cotransfecting 293FT cells (DSMZ, Germany) with the plasmids pHIT60 (gag-pol) and pHIT123 (ecotropic env). Cultivation was performed in high-glucose Dulbecco's modified Eagle's medium (DMEM, Invitrogen) with GlutaMAX containing 10% FBS, 100 IU/ml penicillin, 100 µg/ml streptomycin, 25 mM HEPES, 1 mM sodium pyruvate and 0.1 mM non-essential amino acids. Regular medium were replaced after 16 h by growth medium containing 10 mM sodium butyrate. After an 8-h incubation, the medium was changed back to regular growth medium. 24 h later, the virus supernatant was harvested, filtered through a 0.45-µm filter and loaded by centrifugation (2,000*g*, 90 min at 32 °C) two times on 50 µg/ml RetroNectin-coated (Takara, Madison, WI) nontissue 6-well plates. Three million cells were transduced per well by centrifugation at 600*g* for 30 min and were maintained for 72 h at 37 °C with 5% CO_2 before transfer into culture flasks.

Preparation of bone marrow cells from mice. A complete list of mice used in this study is provided in **Supplementary Table 3**. All mouse experiments were subject to institutional approval by the University of California San Francisco Institutional Animal Care and Use Committee. Bone marrow cells were extracted from mice younger than 6 weeks of age. Bone marrow cells were obtained by flushing the cavities of femur and tibia with PBS. After filtration through a 70-µm filter and depletion of erythrocytes using a lysis buffer (BD PharmLyse, BD Biosciences), the washed cells were either frozen for storage (in 10% DMSO, 90% FBS) or subjected to further experiments.

***BCR-ABL1*–driven mouse model of pre-B ALL and myeloid leukemia.** Bone marrow cells from *Pten*$^{fl/fl}$ (n = 3, female) and *Pten*$^{fl/+}$ (n = 2, female) mice (**Supplementary Table 3**) were collected and retrovirally transformed with a vector expressing *BCR-ABL1*. For B cell lineage leukemia, transduction was performed after culturing bone marrow cells with IL-7 (10 ng/ml) for 1 week. To generate myeloid lineage leukemia, bone marrow cells were cultured with 10 ng/ml recombinant mouse IL-3, 25 ng/ml recombinant mouse IL-6, and 50 ng/ml recombinant mouse stem cell factor (SCF) for 1 week (PeproTech). This treatment leads to selection of hematopoietic progenitor cells ($Lin^-Sca\text{-}1^+c\text{-}Kit^+$ (LSK) cells). Transformation of precursor B cells and LSK cells with the *BCR-ABL1* construct generates pre-B ALL and CML-like models, respectively. After *BCR-ABL1* transduction, all cytokines were removed from the culture to negatively select the nontransduced cells. Both ALL and CML cells were maintained in Iscove's modified Dulbecco's medium (IMDM, Invitrogen) supplemented with GlutaMAX, 20% FBS, 100 IU/ml penicillin, 100 µg/ml streptomycin and 50 µM 2-mercaptoethanol. *BCR–ABL1*–transformed ALL cells were propagated only for short periods of time and usually not longer than 2 months to avoid acquisition of additional genetic lesions during long-term cell culture.

***In vivo* transplantation of leukemia cells.** For *in vivo* experiments, mouse ALL cells were labeled with retroviral firefly luciferase and selected based on antibiotic resistance (blasticidin). The mouse ALL cells were then injected via the tail vein into sublethally irradiated (300 cGy) NOD-SCID recipient mice. Engraftment was monitored using luciferase bioimaging (VIS 100 bioluminescence/optical imaging system; Xenogen). D-luciferin (Xenogen), dissolved in PBS, was injected intraperitoneally at a dose of 2.5 mg/mouse 15 min before measuring light emission. 6- to 8-week-old female NOD-SCID mice (Jackson Laboratories, ME) were randomly allocated into each treatment group. The minimal number of mice in each group was calculated by using the 'cpower' function in the R/Hmisc package. No blinding was used.

C/EBP-α–mediated reprogramming of pre-B cells into myeloid cells. The tetracycline operon–CCAAT/enhancer binding protein alpha–green fluorescent protein (TetO–C/EBP-α–GFP) construct was generated as a modification of the previously published TetO–C/EBP-α–tdTomato lentivirus[27]. *Pten*$^{fl/fl}$ pre-B ALL cells were first transduced with a construct expressing the tetracycline-regulated transcriptional transactivator (rtTA), selected for puromycin resistance and subsequently infected with the TetO–C/EBP-α construct. C/EBP-α was induced in the *Pten*$^{fl/fl}$ pre-B ALL cells by addition of 2 µg/ml doxycycline (Sigma-Aldrich). Staining for cell surface antigens was done with directly conjugated antibodies against CD11b (phycoerythrin (PE)-conjugated; Mac1) and CD19 (PerCP-Cy5.5–conjugated) (EBioscience). To measure the effects of *Pten* deletion in C/EBP-α–reprogrammed pre-B ALL cells, deletion was induced with a tamoxifen-inducible *Cre* or an empty vector control (0.5 µmol/L). The nuclear stain DAPI and 7-aminoactinomycin D (7-AAD) at 1 µg/ml were used as viability markers.

Array-based promoter methylation analysis using HELP. The HELP (HpaII tiny-fragment enrichment by ligation-mediated PCR) assay was performed as previously described[35]. One microgram of high-molecular-weight DNA was digested overnight with isoschizomer enzymes HpaII and MspI, respectively (New England BioLabs (NEB), Ipswich, MA). DNA fragments were purified using phenol-chloroform, resuspended in 10mM Tris-HCl pH 8.0, and used immediately to set up the ligation reaction with MspI-HpaII–compatible adapters and T4 DNA ligase. Ligation-mediated PCR was performed with enrichment for the 200- to 2,000-bp products, and the products were then submitted for labeling and hybridization onto a human HG_17 promoter custom-designed oligonucleotide array covering 25,626 HpaII-amplifiable fragments within the promoters of the genes. For analysis, raw data (.pair) files were generated using NimbleScan software. Signal intensities at each HpaII-amplifiable fragment were calculated as a robust (25% trimmed) mean of their component probe-level signal intensities. Any fragments found within the level of the background MspI signal intensity, measured as 2.5 mean absolute deviation (MAD) above the median of random probe signals, were considered to be 'failed' probes and were removed. A median normalization was performed on each array by subtracting the median log-ratio (HpaII/MspI) of that array (resulting in a median log-ratio of 0 for each array).

Western blotting. Cells were lysed in CelLytic buffer (Sigma, St. Louis, MO) supplemented with phenylmethylsulfonyl fluoride (PMSF), phosphatase and protease inhibitor cocktail (Pierce, Rockford, IL). 15 µg of protein mixture per sample was separated on NuPAGE (Invitrogen, Carlsbad, CA) 4–12% Bis-Tris gradient gels and transferred to PVDF membranes (Immobilion, Millipore, Temecula, CA). For the detection of mouse and human proteins by western blotting, primary antibodies were used together with the WesternBreeze immunodetection system (Invitrogen). Details of the antibodies used are in **Supplementary Table 4**.

Flow cytometry. Antibodies used for flow cytometry experiments are listed in **Supplementary Table 4**. For apoptosis analyses, annexin V, propidium iodide and 7-AAD (BD Biosciences) were used. A Fortessa scanner was used for flow cytometry, and FlowJo v.10 was used for data analysis.

Senescence-associated β-galactosidase assay. Senescence-associated β-galactosidase activity was performed on cytospin preparations. Briefly, a fixative solution (0.25% glutaraldehyde, 2% paraformaldehyde in PBS pH 5.5 for mouse cells) was prepared fresh. 1 g paraformaldehyde was dissolved in 50 ml PBS at pH 5.5 by heating followed by addition of 250 µl of a 50% glutaraldehyde stock solution. 1× X-gal staining solution (10 ml) was prepared as follows: 9.3 ml PBS-$MgCl_2$, 0.5 ml 20× KC solution (820 mg $K_3Fe(CN)6$ and 1,050 mg $K_4Fe(CN)6{\cdot}3H_2O$ in 25 ml PBS) and 0.25 ml 40× X-gal (40 mg 5-bromo-4-chloro-3-indolyl β-D-galactoside per ml of *N*,*N*-dimethylformamide) solutions

doi:10.1038/nm.4062

were mixed. 200,000 cells per cytospin were used (700 r.p.m., 8 min). The fixative solution was pipetted onto cytospins and incubated for 10 min at room temperature, then washed twice for 5 min in PBS-$MgCl_2$. Cytospin preparations were submerged in 1× X-gal solution, incubated overnight at 37 °C in a humidified chamber and washed twice in PBS. Images were acquired using regular microscopy, and the percentage of stained cells was calculated by counting.

Colony-forming assay. Methylcellulose colony-forming assays were performed with 10,000 cells after transformation with *Cre-ER*^{T2} or *ER*^{T2} and 2 d of treatment with 0.5 µmol/liter tamoxifen. Cells were resuspended in murine MethoCult medium (StemCell Technologies, Vancouver, BC, Canada) and cultured on dishes (3 cm in diameter) with an extra water supply dish to prevent evaporation. After 7–14 d, the total number of colonies per plate was counted by microscopy.

Cell cycle analysis. For cell cycle analysis, the BrdU flow cytometry kit for cell cycle analysis (BD Biosciences) was used according to manufacturer's instructions. 5-bromo-2′-deoxyuridine (BrdU) incorporation (APC-labeled anti-BrdU antibodies) was measured along with DNA content (using 7-AAD) in fixed and permeabilized cells. The analysis was gated on viable cells that were identified based on scatter morphology.

Cell-viability assay. 100,000 cells per well were seeded in a volume of 100 µl of medium in Optilux 96-well plates (BD Biosciences, San Jose, CA). Inhibitors were diluted in medium and added at the indicated concentration in a total culture volume of 120 µl. After 3 d in culture, 12 µl of Resazurin (R&D, Minneapolis, MN) was added to each well, and the plates were incubated for 4 h at 37 °C. The fluorescent signal was monitored using 535-nm excitation wavelength and 590-nm emission wavelength. Fold changes were calculated using baseline values of untreated cells as a reference (set to 100%). Each sample was measured in triplicate.

RNA purification and expression analysis. Total RNA was purified using the RNeasy kit (Qiagen, Valencia, CA). RNA quality was checked by using an Agilent Bioanalyzer (Agilent Technologies, Santa Clara, CA). cDNA was generated from 5 µg of total RNA using a poly(dT) oligonucleotide and the SuperScript III Reverse Transcriptase (Invitrogen, Carlsbad, CA). Biotinylated cRNA was generated and fragmented according to the Affymetrix protocol and hybridized to mouse Gene 1.0 ST (Affymetrix, High Wycombe, UK). After scanning (GeneChip Scanner 3000 7G; Affymetrix) of the GeneChip arrays, the generated CEL files were imported to BRB Array Tool (http://linus.nci.nih.gov/BRB-ArrayTools.html) and processed using the RMA algorithm (robust multi-array average) for normalization and summarization. The GEO accession number for the arrays is GSE34829.

Proteomic profiling. Proteomic profiling was performed using reverse-phase protein array (RPPA) analysis[23] on peripheral blood and bone marrow specimens from 192 patients with acute lymphocytic leukemia (ALL), including 192 samples obtained at diagnosis and 12 paired diagnosis-relapse samples, that were evaluated at the University of Texas M.D. Anderson Cancer Center (MDACC) between 1983 and 2007 (two from the 1980s, 45 from the 1990s). Samples were acquired during routine diagnostic assessments in accordance with the regulations and protocols (Lab 01-473 after September 2001, prior protocols for samples before then) approved by the Investigational Review Board (IRB) of MDACC. Informed consent was obtained in accordance with Declaration of Helinski. Samples were analyzed under an IRB-approved laboratory protocol (Lab 05-0654). Samples were selected for inclusion based on availability in the MDACC Leukemia Sample Bank. Patients aged 15 or over were included; another eight pediatric ALL cases were on the array but are not included in this analysis. Samples underwent Ficoll separation to yield a mononuclear fraction. The samples were normalized to a concentration of 1×10^4 cells/µl and a whole-cell lysate was prepared as previously described[28]. All protein samples were prepared from fresh cells on the day of collection. Of the 192 newly diagnosed ALL cases, most were treated with the hyper CVAD (cyclophosphamide, vincristine, adriamycin and dexamethasone) regimen either alone ($n = 91$) or in combination with rituximab ($n = 31$), a tyrosine kinase inhibitor ($n = 28$) or nelarabine ($n = 3$). A modification of the Berlin-Frankfurt-Mannheim regimen was used in 23 cases. The remaining 16 cases received miscellaneous combination regimens that were in use over this time period.

Glucose, lactate and ATP measurements. Glucose and lactate levels were measured using the Amplex Red Glucose/Glucose Oxidase Assay Kit (Invitrogen) and the L-Lactate Assay Kit (Cayman Chemical), respectively, according to the manufacturers' protocols. Glucose and lactate concentrations were measured in fresh and spent medium. Total ATP levels were measured using the ATP Bioluminescence Assay Kit CLS II (Roche) according to the manufacturer's protocol. 10^6 cells/ml were seeded in fresh medium and treated as indicated in the figure legends. The relative levels of glucose consumed and lactate produced, and the total amount of ATP, are shown, and all values were normalized to the number of viable cells. Inhibitors used in this study are listed in **Supplementary Table 5**.

Reconstitution model for pre-BCR signaling. Pre-B cells from *Blnk*$^{-/-}$*Rag2*$^{-/-}$*Igll1*$^{-/-}$ triple-knockout transgenic mice[26] were engineered to express a non-autoreactive pre-BCR (µ-HC^{NA}), an autoreactive pre-BCR (µ-HC^{Auto}) or an empty-vector control (EV). The cells were transduced with a tamoxifen-inducible (*Blnk*-ER) form of the pre-BCR linker molecule Blnk (also known as SLP-65). Addition of tamoxifen (Tam) releases Blnk from its complex with heat-shock protein (HSP) 90 and allows for assembly of the pre-BCR signaling complex within minutes.

Statistical analysis. Unpaired, two-tailed Student's *t*-tests were used to compare colony number, S phase percentage and frequency of cellular senescence between different groups. A two-sided Mann-Whitney-Wilcoxon test was used to compare methylation values of ALL versus normal pre-B or B-cell lymphoma groups and RPPA data of newly diagnosed adult ALL versus T cell lineage ALL or mature B cell lymphoma, using R version 2.14.0. The Mantel-Cox log-rank test (two-sided) was used to compare survival data between different groups. R package 'survival' version 2.35-8 was used for the survival analysis.

35. Khulan, B. *et al.* Comparative isoschizomer profiling of cytosine methylation: the HELP assay. *Genome Res.* **16**, 1046–1055 (2006).